ELSEVIER

Contents lists available at ScienceDirect

# Ceramics International

journal homepage: www.elsevier.com/locate/ceramint





# Synthesis and polishing characteristics of a novel green GO/diamond hybrid slurry under ultrasonic technology

Xin Chen <sup>a,b</sup>, Yingdong Liang <sup>a,b</sup>, Zhijie Cui <sup>a,b</sup>, Chao Zhang <sup>a,b</sup>, Zixuan Wang <sup>a,b</sup>, Tianbiao Yu <sup>a,b,\*</sup>, Ji Zhao <sup>a,b,\*\*</sup>

- <sup>a</sup> School of Mechanical Engineering and Automation, Northeastern University, Shenyang, 110819, China
- b Liaoning Provincial Key Laboratory of High-end Equipment Intelligent Design and Manufacturing Technology, Northeastern University, Shenyang, 110819, China

#### ARTICLE INFO

Keywords:
Graphene oxide/diamond hybrid slurry
Ultrasonic polishing
Lubrication
Silicon carbide
Graphene oxide

#### ABSTRACT

Ultrasonic polishing (UP), as an efficient and clean precision machining process, is increasingly applied in the hard and brittle material processing. To minimize the surface damage and polishing expenses, this paper aims to prepare novel graphene oxide/diamond hybrid slurries (GDS) by ultrasonication, and to investigate the UP mechanisms for silicon carbide (SiC) ceramics on UP and tribological experiments. Findings showed that GDS exhibited superior polishing performance compared to diamond polishing slurries. Moreover, the promotion effect of GDS was more obvious under UP. The surface roughness was improved by 31.62% after UP using GDS with a graphene oxide (GO) content of 0.1 wt%. On the one hand, the lubrication of GO reduce the wear and coefficient of friction. On the other hand, ultrasonic vibration induces stronger impact kinetic energy of abrasives to remove material and allows for a better uniform distribution of GDS to further enhance the lubrication characteristics of GO nanosheets. The application of GO in UP is a processing technology penetrating the manufacturing industry and even human life, laying the foundation for SiC nano-polishing.

#### 1. Introduction

Currently, traditional polishing processing for hard and brittle ceramic materials suffers from notable defects, such as severe scratches, extensive brittle fractures, sub-surface damage, frosting phenomena, etc., which manifestly fail to meet the functional and performance requirements of the existing industry [1-3]. Moreover, the extraordinary hardness and wear resistance of ceramics continue to limit the further improvement of polishing efficiency and quality [4]. Along with the advent of ultrasonic technology in the manufacturing industry, ultrasonic polishing (UP), as an efficient and clean precision machining process, has obtained satisfactory outcomes in the field of hard and brittle optical material processing [5-7]. To address the problems encountered with low polishing efficiency and quality, Zhao et al. [8] applied ultrasonic vibration technology to cylindrical surface polishing of SiC ceramic to investigate the interaction behavior between the material and tool. The results showed that the frictional resistance and surface roughness reduced with the introduction of ultrasonic vibration.

Zhang et al. [9] conducted axial UP experiments on BK7 glass. The research results indicated that the polishing performance increased significantly with increasing ultrasonic amplitude. Compared to the case without ultrasonic vibration, the material removal rate (MRR) increased by 29.07% and the surface roughness decreased by 28.85% when the amplitude was  $10 \, \mu m$ . Zhai et al. [10] combined ultrasonic vibration and magnetorheological polishing to further enhance the MRR of sapphire wafer. The MRR increased by approximately 3.4 times compared to ordinary magnetorheological polishing. Based on the vibration effect, Ge et al. [11] proposed an ultrasonic-assisted soft abrasive flow (SAF) method to target the low removal efficiency owing to turbulent layer separation. The findings indicated that ultrasonic vibration effectively improved the SAF polishing accuracy and efficiency without generating cavitation erosion. Yang et al. [12,13] developed ultrasonic assisted electrochemical mechanical polishing (UAECMP) used for 4H-SiC (0001) wafers. The findings showed that ultrasonic vibration significantly enhanced the anodic oxidation of 4H-SiC. Moreover, the MRR of UAECMP reached 14.54 μm/h, approximately 4.5 times higher than that of conventional electrochemical mechanical polishing (ECMP).

<sup>\*</sup> Corresponding author. School of Mechanical Engineering and Automation, Northeastern University, Shenyang, 110819, China.

<sup>\*\*</sup> Corresponding author. School of Mechanical Engineering and Automation, Northeastern University, Shenyang, 110819, China. E-mail addresses: northeastern\_cx@163.com (X. Chen), 1910112@stu.neu.edu.cn (Y. Liang), 2110122@stu.neu.edu.cn (Z. Cui), 1910116@stu.neu.edu.cn (C. Zhang), wangzx@mail.neu.edu.cn (Z. Wang), tbyu@mail.neu.edu.cn (T. Yu), jzhao@mail.neu.edu.cn (J. Zhao).

Nomenclature		t	Polishing time
		MP	Mechanical polishing
UP	Ultrasonic polishing	DPS	Diamond abrasives polishing slurry
GDS	Graphene oxide/diamond hybrid slurries	ECMP	Electrochemical mechanical polishing
UAECMP	Ultrasonic assisted electrochemical mechanical polishing	MRR	Material removal rate
SAF	Soft abrasive flow	wt%	Weight concentration
SiC	Silicon carbide	0.075GD	S GDS with a GO content of 0.075 wt%
0.025GD	S GDS with a GO content of 0.025 wt%	0.1GDS	GDS with a GO content of 0.1 wt%
0.05GDS	GDS with a GO content of 0.05 wt%	DI	Deionized
GO	Graphene oxide	3D	Three-dimensional
2D	Two-dimensional	COF	Coefficient of friction
CNC	Computer numerical control	CLSM	Confocal laser scanning microscope
SEM	Scanning electron microscopy	n	Spindle speed
$W_{ m GO}$	GO content	R	Polishing tool radius
$W_{\rm a}$	Abrasives content	$ u_{ m w}$	Feed rate
Α	Ultrasonic amplitude	$X_{\mathrm{d}}$	Average abrasives size
f	Ultrasonic frequency	$\boldsymbol{X}$	Reciprocation distance
d	Pre-compressed distance	$\nu_{ m z}$	Vertical vibration speed of polishing tool
z	Vertical vibration position of polishing tool	$arphi_0$	Initial phase of ultrasonic system
$z_0$	Initial vertical vibration position of polishing tool		

Unfortunately, ultrasonic vibration also increased the surface roughness of the polished surface.

Ultrasonic polishing technology has reached an outstanding level in the field of ultra-precision manufacturing of difficult-to-machine materials. Yet, polishing is a time-consuming and accurate process. Ultrasonic systems operating for long periods inevitably generate high volumes of heat whilst affecting the service life of the machine [14]. Therefore, in order to minimize the damage and polishing expenses during the high-quality ceramic surfaces processing in such a complex UP system, the reduction of frictional wear in the machining area becomes a critical requirement in the manufacturing industry, where excessive wear could lead to additional sample damage and device malfunction [15,16]. Nano-lubrication technology is regarded as one of the effective methods of achieving high efficiency and quality surface machining and extending the lifetime of machine tools [17]. Hybrid nanofluids are widely used in the manufacturing and automotive polishing fields owing to the potential to significantly offer lubricity for the machined area while accelerating material removal [18,19]. The early common formulations of MP slurry generally included one type of abrasive particles, such as diamond or cerium oxide [20]. Driven by the incessant pursuit of nanofluids with more desirable properties, Jana et al. [21] first investigated hybrid nanofluids in 2007. In recent years, to achieve ultra-smooth polished surfaces in the aerospace industry, nanoscale solid particles were added into conventional base fluids to improve the lubrication and processing characteristics of novel nano-polishing fluids. Therefore, developing an eco-friendly and lubricated hybrid slurry is critical for the production of high-precision optical mirrors at low costs.

To date, carbon-based nanoparticle materials, typically dispersed as additions into nanofluids, exhibited different lubrication features [16, 22,23], such as nanoscale diamond particles, graphene nanoparticles, graphite fluoride, graphene oxide (GO) nanosheets, carbon nanotubes and fullerenes. Due to the unique two-dimensional (2D) nano lamellar structure, high specific surface area and abundance of functional groups on the surface, GO enables a good enhancement of the lubricity of synergistic suspensions [23]. For instance, Li et al. [24] prepared GO coolants for ultra-precision grinding of  $Gd_3Ga_5O_{12}$  crystals, which resulted in a significantly improved ground surface quality than ionized water coolant due to its reduced abrasive-substrate interfacial friction. Yi et al. [25] found that drilling of titanium alloy with GO suspensions effectively reduced the value of surface roughness, tool wear, and coefficient of friction in comparison to conventional drilling. Li [26] et al.

formulated GO nanosheets coolants for cutting titanium alloy, which enabled the reduction of both cutting temperature and friction force compared to conventional coolant. Huang et al. [27] systematically evaluated the polishing performance of a water-based nanosuspension using diamond particles and GO nanosheets as additives in terms of oxidation, lubrication, and removal characteristics, and the results showed that diamond/GO hybrid nanosuspensions not only improved the removal efficiency, but also enhanced the polished surface quality. Furthermore, since GO is a non-toxic, green and renewable resource with low environmental impact, polishing with GO lubrication can avoid poor surface accuracy and severe surface damage, whilst not causing serious environmental pollution issues. In addition, the flaws of GO are surrounded by epoxide and hydroxyl groups, while the edges are modified by carboxyl groups [28]. During material removal, GO nanosuspensions increase the masses of active sites and free radicals for chemical reaction to accelerate the softening of machined surface and made it easier to be mechanically removed [29,30]. Apparently, GO-enhanced hybrid suspensions have exhibited promising practical applications in processing. However, the utilization of GO nanomaterials combining the diamond abrasives as hybrid slurries has remained under-reported in the ultrasonic polishing mechanism research, especially in the field of ceramic polishing.

In this paper, water-based GO nanofluids were prepared by ultrasonication, and the optimum ultrasonication time for the uniformity was revealed based on ultraviolet–visible spectroscopy. Subsequently, novel GO/diamond hybrid slurries were synthesised by dispersing the GO nanofluids into diamond polishing base fluids. Ultrasonic polishing experiments were also carried out with different weight percent concentrations of GO and ultrasonic amplitudes on SiC ceramics. Through analyzing the polishing and wear surfaces, the ultrasonic polishing mechanisms of GO/diamond hybrid slurries were revealed in terms of lubrication and mechanical removal.

# 2. Methodology

# 2.1. Preparation of GO/diamond hybrid slurries

The industrial grade monolayer GO nanosheets, supplied by Suzhou Tanfeng Graphene Tech. Co., Ltd., were used as nano-additives for the preparation of GO nanofluids. The X-ray diffraction spectra of GO nanosheets is shown in Fig. S1 in the Supplementary Information. Table 1 shows the detailed properties of GO nanosheets. Due to the high

**Table 1**The properties of GO nanosheets used in this paper.

Property	Value	
Layer	1–2	
Purity	90%	
Thickness	3–8 nm	
Lateral size	0.2–50 μm	
Appearance	Dark brown sheet	
Thermal conductivity	5300 W/(m·K)	

surface area of nanoparticles, the agglomeration or adsorption of other particles easily occurs, resulting in the deterioration of the specific surface properties [31]. In order to achieve non-clustering and uniform dispersion of GO, ultrasonic dispersion is one of the eco-friendly, effective, time-saving and economical alternatives for improving the dispersion stability of nanofluids [32], breaking the agglomeration of nanoparticles and exfoliating them homogeneously in the fluid through the sonication-induced cavitation effect [33]. A three-step method was established to prepare GO/diamond hybrid slurries. Firstly, 0.25 g of graphene oxide and 100 g of deionized (DI) water were weighed and mixed, then magnetically stirred for 30 min at 500 rpm. Secondly, an intensive ultrasonic probe (Biosafer 1800–99) with a 20 mm diameter variable amplitude rod was used to agitate GO nanofluids at 20 kHz, as displayed in Fig. 1(i). Due to the degradation of GO above 38 °C, the temperature was controlled at 30 °C during the preparation process. An

ice-water bath was also adopted for constant temperature control, and the ultrasonic process was pulsed at 360 W with 2 s ON and 5 s OFF to prevent the fluid temperature from rising too quickly. The ultrasonication time of the GO was set to 90 min according to Fig. S2. The SEM images of GO in Fig. 1(a–c) displays that the lateral size of the origin GO is approximately dozens of microns, and it has some wrinkles on surface. After ultrasonic dispersion, the size of GO reduces to approximately hundreds of nanometers, and it presents a thin and smooth laminated structure with no small wrinkles, as shown in Fig. 1 (d). Thus, the GO used in this paper is a few-layer structured nanomaterial, which is expected to achieve lubrication function in the polishing slurries. Thirdly, GO nanofluids and DI water were added in proportion to the diamond base fluids, and then sonicated for 30 min to obtain GO/diamond hybrid slurries (GDS) with four GO concentrations, as shown in Table 2. The diamond base fluid used in this paper was an

**Table 2**Percentage of diamond and graphene oxide of the prepared hybrid slurries.

Group No.	Diamond content (wt%)	GO content (wt%)
1	15	0
2		0.025
3		0.05
4		0.075
5		0.1

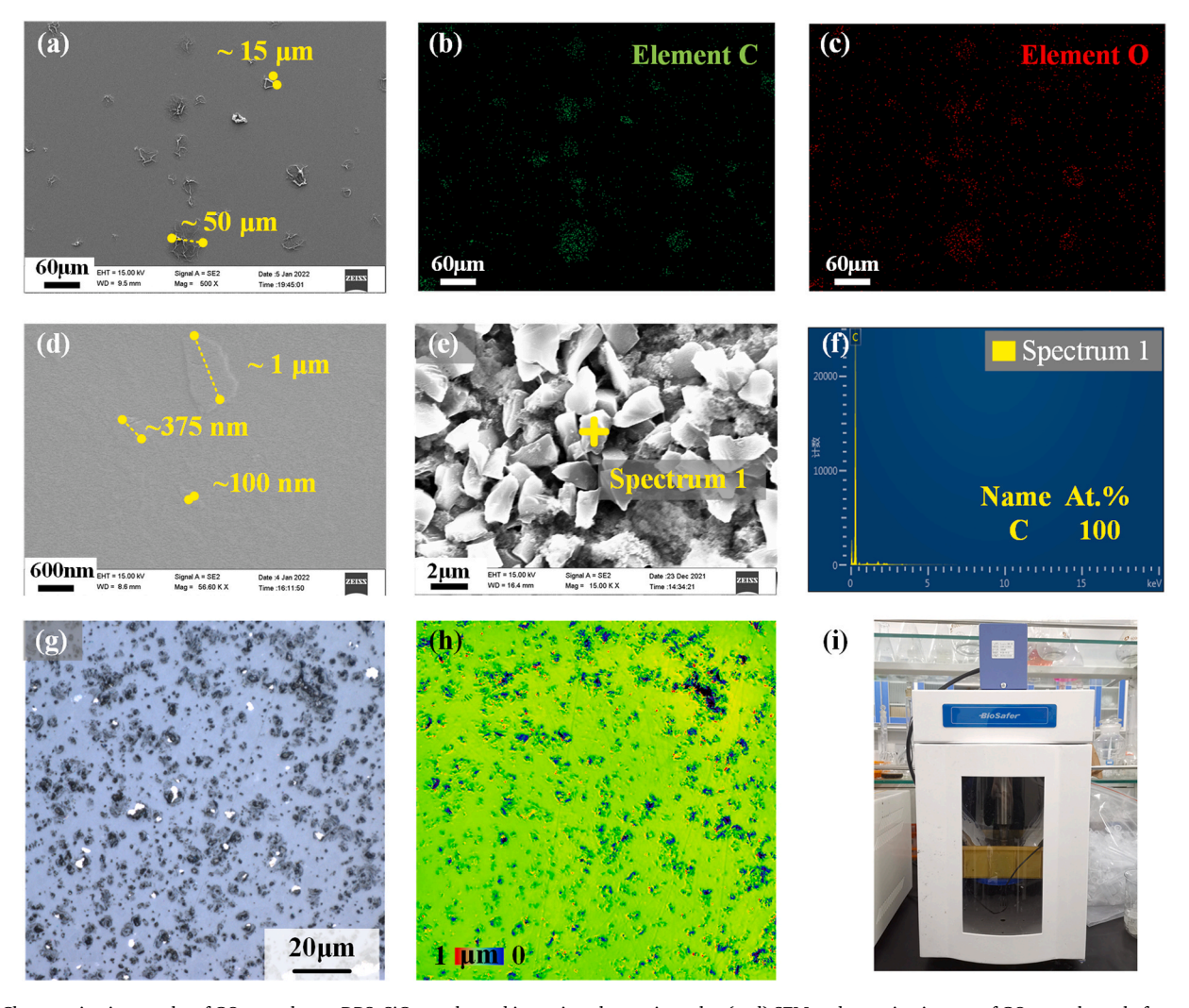


Fig. 1. Characterization results of GO nanosheets, DPS, SiC sample, and intensive ultrasonic probe: (a–d) SEM and mapping images of GO nanosheets before and after ultrasonication; (e–f) SEM and spectrum images of DPS; (g–h) CLSM images of SiC; (i) Image of intensive ultrasonic probe.

advanced diamond abrasives polishing slurry (DPS) supplied by Xin Hui Electronic Technology Co., Ltd. The SEM image of DPS in Fig. 1(e–f) depicts that the diamond particles with an average particle size of 1.5  $\mu$ m are uniformly distributed and sharp-edged.

#### 2.2. Ultrasonic polishing experimental setup

In order to explore the effect of GO content in GDS and ultrasonic amplitude on the surface roughness and MRR, 10 groups of surface polishing experiments were conducted on a self-built 5-axis computer numerical control (CNC) polishing machine tool, as shown in Fig. 2. Wool-type polishing tools with a diameter of 4 mm were used to achieve material removal. The wool polishing tool fixed on the ultrasonic spindle rotated at 6000 rpm and reciprocated at a lateral feed rate of 2 mm/s over a distance of 12 mm, as shown in Table 3. The SiC samples with a size of 50 (length)  $\times$  50 mm (width)  $\times$  8 mm (height) were fixed in the polishing sink and a force dynamometer (Kistler 9257 B) was clamped at the sink bottom for the calibration and measurement of the polishing force. The CLSM images in Fig. 1(g-h) reveals that the as-received surface of the SiC sample has numerous surface defects (pits and bulges) with a surface roughness Sa of 85 nm. Each GDS was used for two groups of polishing experiments with ultrasonic amplitudes of 0 and 6  $\mu m$ respectively.

## 2.3. Tribological experimental setup and surface characterization

To further evaluate the lubrication performance of GDS, the tribological properties of samples under different GO lubrication conditions were measured using a ball-on-block reciprocating friction and wear tester (MFT-4000), as shown in Fig. 3. The 5 mm diameter SiC ceramic balls were used to reciprocally scratch SiC samples with the size of 30 mm (length)  $\times$  30 mm (width)  $\times$  4 mm (height) under a load force of 10 N, a reciprocating distance of 5 mm and a speed of 200 mm/min for 30 min. Before the frictional wear experiments, the SiC samples were polished to flatten the surface. Then, the wear area shown in Fig. 3(b) was defined.

Before/after the tribological and polishing experiments, the samples were ultrasonically cleaned in alcohol and DI water bath for 20 min and dried at 40 °C for 20 min to remove any contaminants. Field emission scanning electron microscopy (SEM, ZEISS ULTRA PLUS) was employed to determine the morphology of GO and diamonds, and a confocal laser scanning microscope (CLSM, OLS4100) was employed to inspect the sample machined surface and measure the MRR and surface roughness.

**Table 3**Ultrasonic polishing experimental conditions.

Experimental conditions	Parameters	
GO content, W <sub>GO</sub> (wt%)	0, 0.025, 0.05, 0.075, 0.1	
Abrasives content, $W_a$ (wt%)	15	
Ultrasonic amplitude, A (μm)	0, 6	
Ultrasonic frequency, $f$ (kHz)	25	
Pre-compressed distance, d (mm)	0.05	
Polishing time, t (s)	1800	
Spindle speed, n (rpm)	6000	
Polishing tool radius, R (mm)	4	
Feed rate, $v_w$ (mm/s)	2	
Average abrasives size, $X_d$ (µm)	1.5	
Reciprocation distance, X (mm)	12	

#### 3. Results and discussion

## 3.1. Polishing characteristics of GO/diamond hybrid slurries

Fig. 4 displays the surface roughness and MRR of SiC samples polished by mechanical polishing (MP) and UP using the DPS and four types of GDS. As shown in Fig. 4(a), for the DPS, the surface roughness of polished SiC sample was 26.6 nm in MP, while the addition of ultrasonic vibration increased the surface roughness to 27.2 nm in UP. In comparison, the polished SiC surfaces using GDS was significantly superior to those polished using DPS. The GDS with GO contents of 0.025, 0.05, 0.075, 0.1 wt% are assigned as 0.025GDS, 0.05GDS, 0.075GDS and 0.1GDS, respectively. During the MP using 0.025GDS, 0.05GDS, 0.075GDS and 0.1GDS condition, the surface roughness was 24, 23, 22.8, 20 nm, respectively, which was decreased by 9.77%, 13.53%, 14.29%, and 24.81% relative to the DPS condition. During the UP using 0.025GDS, 0.05GDS, 0.075GDS and 0.1GDS condition, the surface roughness was 25, 23.2, 19.4, 18.6 nm, respectively, which was decreased by 8.09%, 14.71%, 28.67%, and 31.62% relative to the DPS condition. Meanwhile, Fig. 5 exhibits the 2D and three-dimensional (3D) surface morphology of SiC ceramic polished by MP and UP under DPS and four types of GDS. The polished surface exhibited the plastic scratching behaviour of diamond abrasives to remove material. The defects such as furrows, protrusions, small cracks and holes on the sample surface indicated that most material removal was completed in the plastic state. In particular, the polished surface using DPS showed an obvious fluctuation in Fig. 5(a and b). During the four GDS conditions, the scratches phenomenon was significantly reduced. The 3D surface morphology in Fig. 5 shows that the addition of GO improved the

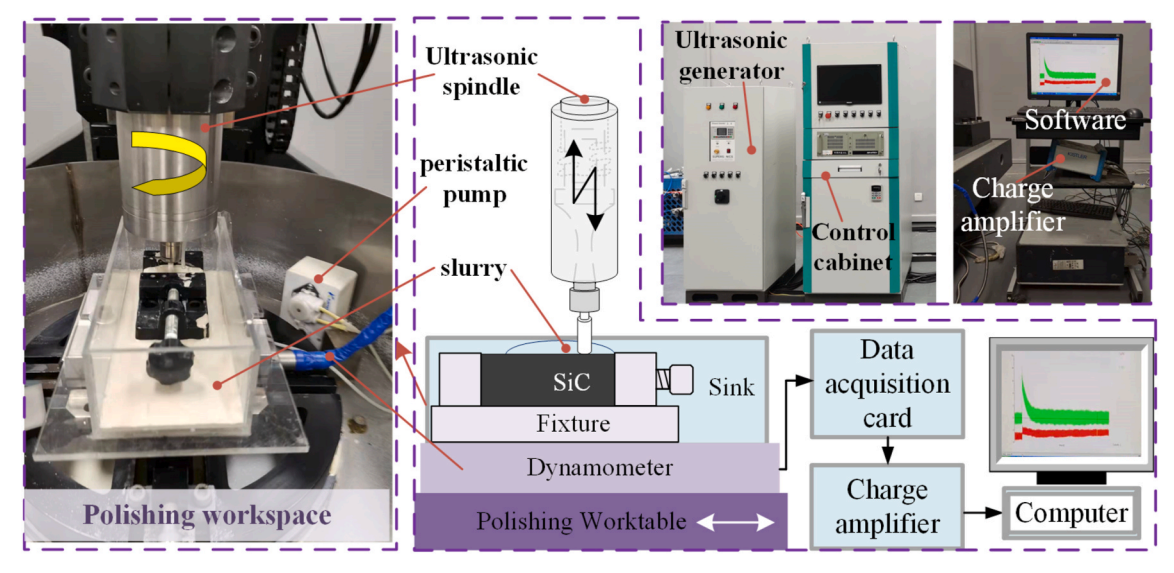


Fig. 2. Illustration of ultrasonic polishing system.

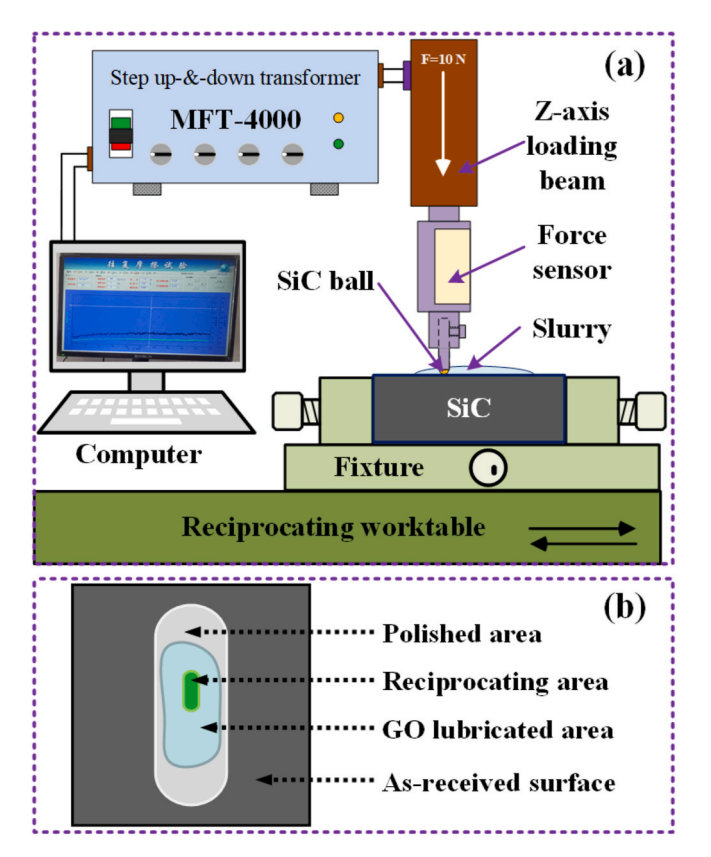
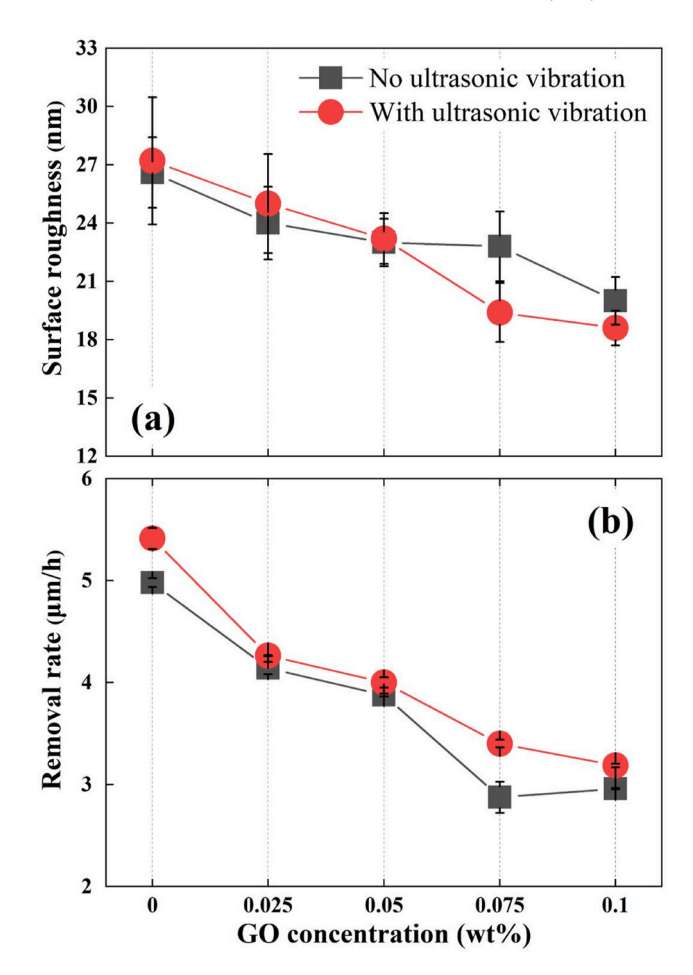


Fig. 3. (a) Schematic of tribological experimental setup, (b) the definition of wear area.

polished surface quality. As the GO concentration increased, the scratches on the 3D morphology were significantly reduced, and the size and amount of small holes on the 2D morphology was smaller, meanwhile the polished surface was smoother. Especially in the 0.1GDS condition, a relatively smooth machined surface was clearly observed in Fig. 5(i and j).

The surface roughness and quality in the four GDS conditions were superior relative to the DPS condition. Meanwhile, the increasing GO concentration resulted in a smaller surface roughness and better surface quality. It was probably mainly because more GO nanosheets allowed for better lubrication in the polished area, which could lower the coefficient of friction (COF), ploughing intensity and microcutting force, and better the surface quality [34]. Furthermore, by comparing MP and UP, it can also be found that the using of ultrasonic vibration deteriorated surface quality when GO concentration was less than or equal to 0.05 wt %, but the surface quality was improved with ultrasonic vibration when GO concentration was greater than 0.05 wt%. The surface roughness improvement reached a maximum of 31.98% under the GDS condition combining ultrasonic vibration and 0.1 wt% GO. This was likely attributed to the lower ploughing intensity, as ultrasonic vibration effectively provided better flow, uniformity and lubrication properties of GDS [35].

As shown in Fig. 4(b), the MRR of polished SiC sample using the DPS in MP and UP conditions were 4.978 and 5.413  $\mu m/h$ , respectively. Apparently, the MRRs of SiC samples polished by GDS were lower than those of the samples polished by DPS for both MP and UP, and the MRR decreased with increasing GO content. During the 0.1GDS condition, the MRR in MP and UP conditions were 2.959 and 3.186  $\mu m/h$ , reaching a maximum decrease rate of 40.56% and 41.13% relative to the DPS condition. This may be attributed to the fact that more GO nanosheets could produce an improved lubrication between the abrasives and workpiece [27]. Furthermore, ultrasonic vibration contributed effectively to increasing the MRR of the SiC polishing process. The maximum



**Fig. 4.** Material removal rate (a) and surface roughness (b) of the SiC polished by MP and UP under DPS and four types of GDS.

increment of removal rate reached 18.3% under GDS condition with a GO concentration of 0.075 wt%. It could be principally because the ultrasonic tool endowed with a high-frequency vibration energy increased the relative linear velocity of diamond abrasives, which enhanced the removal rate [36,37]. Moreover, the ultrasonic-induced cavitation of the polishing solution also has a slight ameliorating function, albeit this is relatively weak [38].

# 3.2. UP mechanism analyses of GO/diamond hybrid slurries

The UP of SiC using GO/diamond hybrid slurries is a complicated process in which GO lubrication and abrasives mechanical removal complement and facilitate each other. Tribological behaviors are an important characteristic to reveal the lubrication properties of GO during SiC polishing, which can be evaluated by the COF, wear profiles (wear depth) and wear morphology (wear width and wear area). Fig. 6 shows the COF curves with time of different samples using DPS and GDS with four different GO concentrations. It shows that the COF value in liquids was relatively stable except for the initial stages. The curve data from the last 10 min were used to calculate the average COF at steady stage with different GO lubrication. The COF value of difference samples follow the given order: DPS >0.025GDS >0.05GDS >0.075GDS >0.1GDS. For DPS, the COF showed a maximum value of 0.389. The COF under the other four GDS were all significantly lower than that under the DPS. And the value of the COF decreased as the GO concentration increased. When the GO concentration was 0.1 wt%, the average COF decreased to 0.340, which was 0.874 times of DPS and 0.919 times of 0.025GDS. This also reveals that effective GO can properly modify the friction between samples.

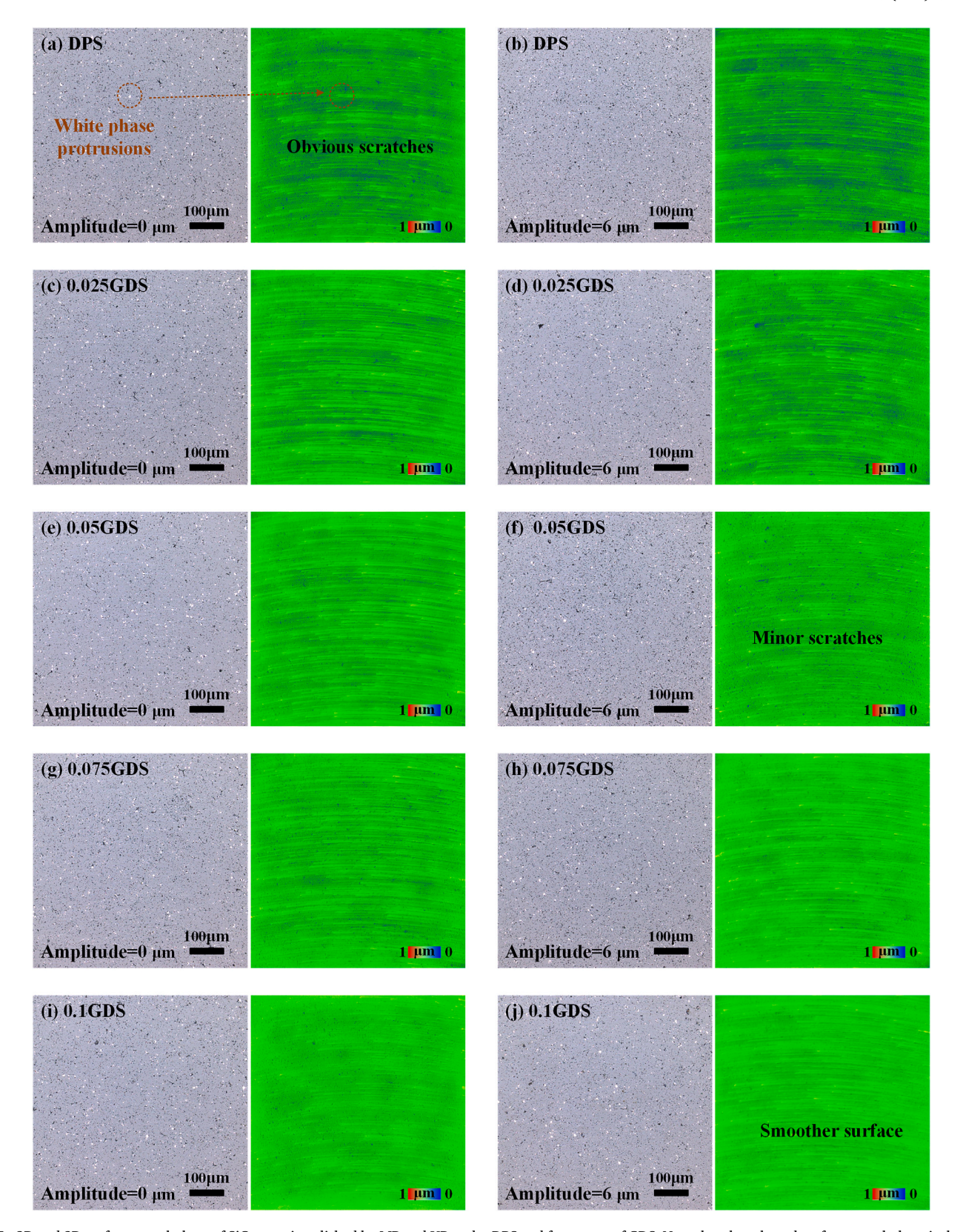


Fig. 5. 2D and 3D surface morphology of SiC ceramic polished by MP and UP under DPS and four types of GDS. Note that the selected surface morphology is the most representative and sufficient to express the tendency with increasing GO concentration.

Fig. 7 shows the cross-section profiles, wear depth and wear area of samples using DPS and GDS with four different GO concentrations acquired from Fig. S3. The sample under DPS showed largest wear depth and wear area of  $5.415~\mu m$  and  $2880~\mu m^2$  respectively. As expect, the

samples under GDS displayed a smaller profile, indicating that smaller depths and areas were removed by the grinding ball. In addition, as the increase of GO concentration in GDS, the wear depth and wear area constantly decreased. When 0.1 GDS was used, the minimum wear depth

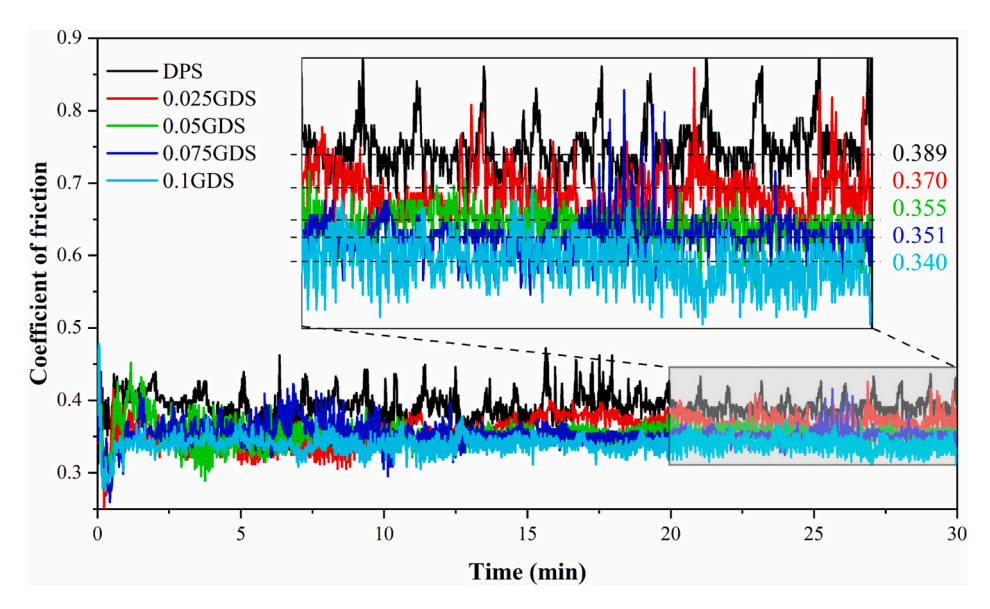


Fig. 6. Coefficient of friction curves with time of different samples using diamond polishing slurry and GO/diamond hybrid slurries with four different GO concentrations.

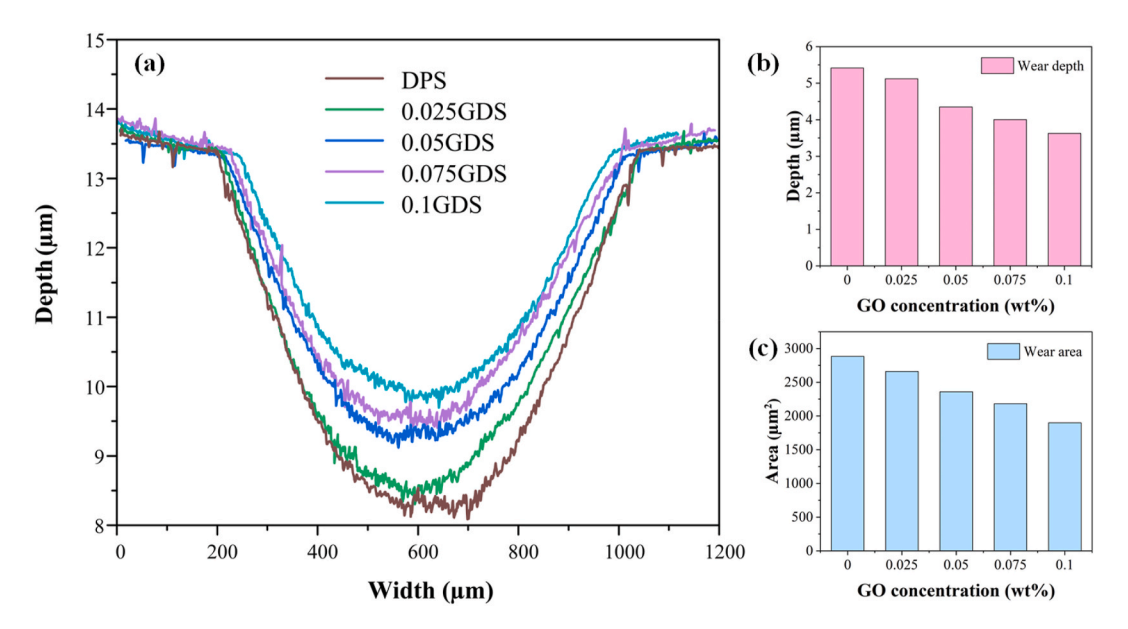


Fig. 7. (a) The cross-section profiles, (b) depth and (c) area of wear samples using diamond polishing slurry and GO/diamond hybrid slurries with four different GO concentrations.

was 3.628  $\mu m$ , which was 0.670 times that of DPS, and the minimum wear area was 1900  $\mu m^2$ , which was 0.660 times that of DPS.

The 2D local morphologies of wear samples and grinding balls using DPS and GDS with four different GO concentrations were shown in Figs. 8 and 9. Majority of the machined surfaces of grinding balls and wear samples presented the microcutting removal-induced uniform scratches phenomenon in the plastic zone, which was fundamentally created by the abrasive wear of diamond abrasives in the wear area under lubricated conditions. The wear morphology of wear samples and grinding balls in Figs. 8(a) and 9(a) exhibit the presence of the widest scratches and largest removal under DPS. Apparently, better areal lubrication properties were found in GDS with more GO nanosheets. A higher GO content of GDS left a narrower wear track and smaller wear ball area, which explained the minimal SiC polishing rate in the GDS condition at high concentrations, as shown in Figs. 8(e) and 9(e). Thus, more GO nanosheets within a reasonable range were advocated in

manufacturing processes that ultimately seek high-precision surfaces with trace removal.

According to the above results, the promotional mechanism of ultrasonic vibration and GO nanosheets in SiC polishing is shown in Fig. 10. During the conventional MP in Fig. 10(a), the sample surface is mainly polished by the scratching action of diamond abrasives to plough and remove the material. A few scratches and pits are left on the polished surface, as shown in Fig. 5(a) of the experimental results. Fig. 10 (b) depicts the UP using DPS process. Compared to conventional MP, UP uses ultrasonic vibration energy to provide diamond abrasives in DPS with stronger impact kinetic energy. The high frequency of vibration brings the abrasive a larger movement range and a higher cutting speed [39], as shown in Eqs. (1) and (2), thereby removing more SiC samples and leaving deeper scratches and pits.

$$z = z_0 + A\sin(2\pi f t + \varphi_0) \tag{1}$$

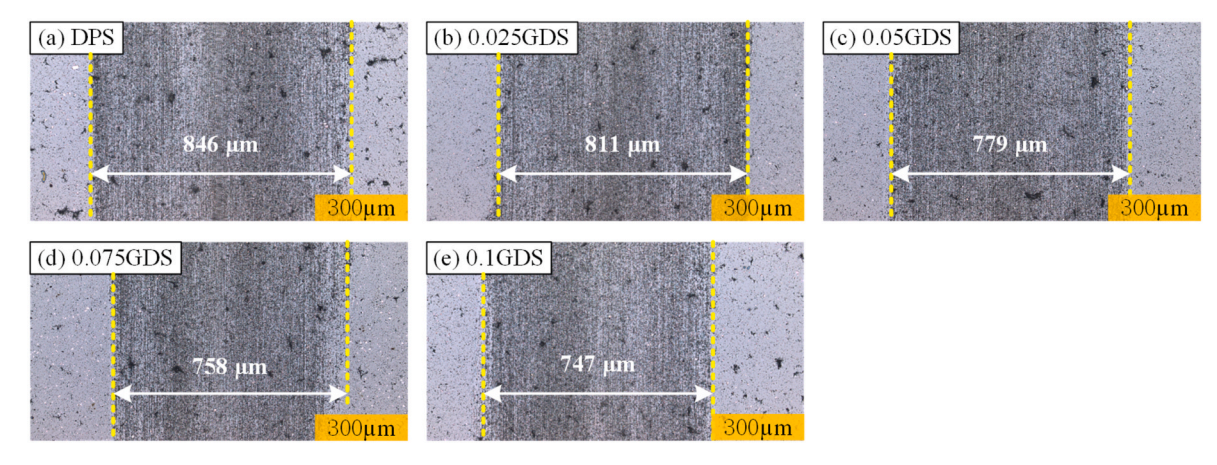


Fig. 8. 2D local morphology of wear samples using diamond polishing slurry and GO/diamond hybrid slurries with four different GO concentrations.

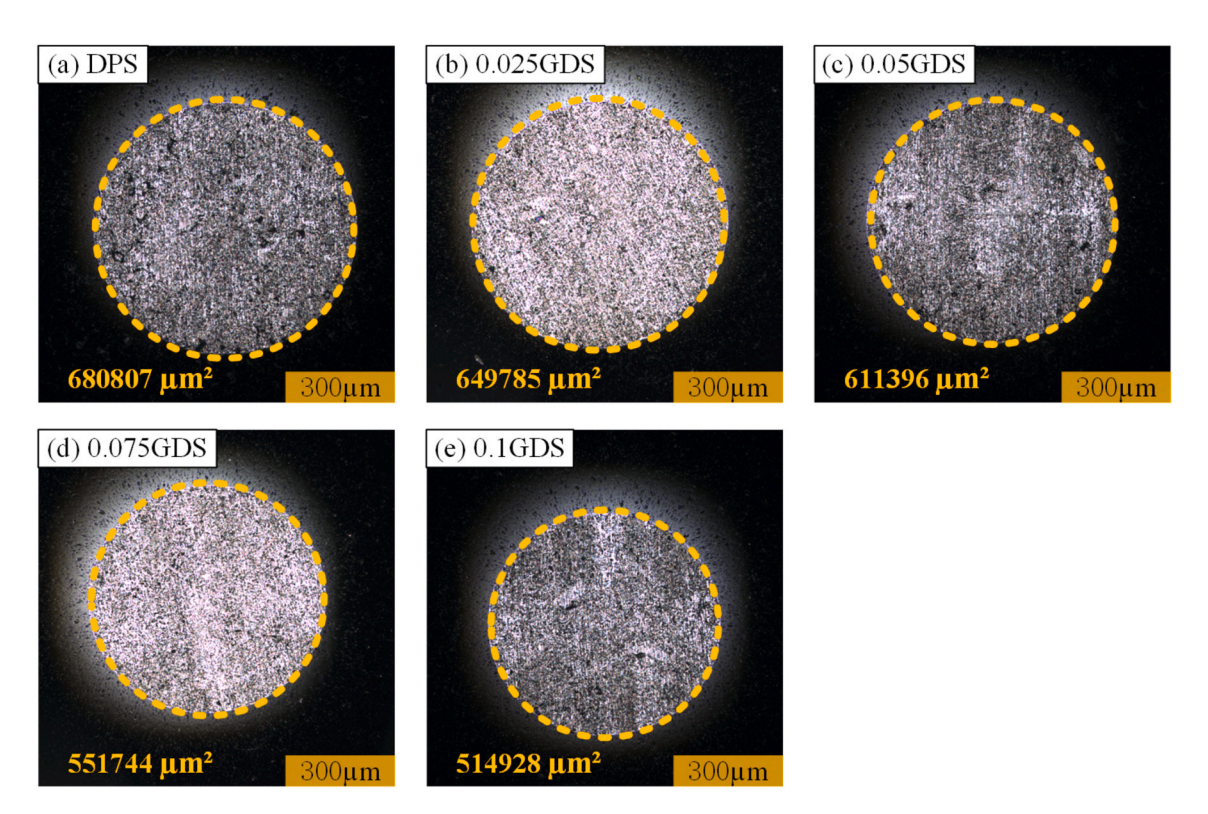


Fig. 9. 2D morphology of grinding balls using diamond polishing slurry and GO/diamond hybrid slurries with four different GO concentrations.

$$v_z = 2\pi A f \cos(2\pi f t + \varphi_0) \tag{2}$$

where z and  $v_z$  are the vertical vibration position and speed of polishing tool, A and f are the ultrasonic vibration amplitude and frequency of ultrasonic system, respectively,  $z_0$  is the initial vertical vibration position of polishing tool,  $\varphi_0$  is the initial phase of ultrasonic system.

Fig. 10(c) exhibits the MP using GDS process. The addition of GO can strengthen the lubrication performances of slurries with respect to the wear-resisting and friction-reducing. GO nanosheets are penetrated between the polishing tool, diamond abrasives and sample surface to form a microscopic 'bearing-like' structure, and the formation of which can not only enhance the wetting performance of the diamond base slurry, also reduce the aggregation of diamond abrasives [40,41], which in turn reduces wear during machining. Fig. 10(d and e) exhibits the UP using GDS process. GO lubrication performances are also present in UP of SiC. Ultrasonic vibration not only directly induces an accelerated impact of diamond abrasives, but also allows for a more uniform distribution of

GO and abrasives to further enhance the lubrication characteristics of GO nanosheets, as shown in Fig. S4. Diamond abrasives can be induced by GO nanosheets and ultrasonic vibration to establish a better SiC surface compared to polishing using DPS. Moreover, the coupling of ultrasonic vibration and GO is even more dramatic in improving the polishing surface quality, and this is even more evident in GDS with high concentrations of GO, as shown in Fig. 5. The GDS of more GO nanosheets exhibits excellent lubricating performances, improves the lubricating state during the polishing region, lower the COF, wear force, and ploughing intensity of abrasives, thereby obtaining a smaller material removal depth and a smoother surface in SiC polishing [42].

## 4. Conclusions

In this paper, water-based GO nanofluids and GO/diamond hybrid slurries were prepared by ultrasonication method for high precision ultrasonic polishing of SiC optical mirror materials. GO/diamond hybrid

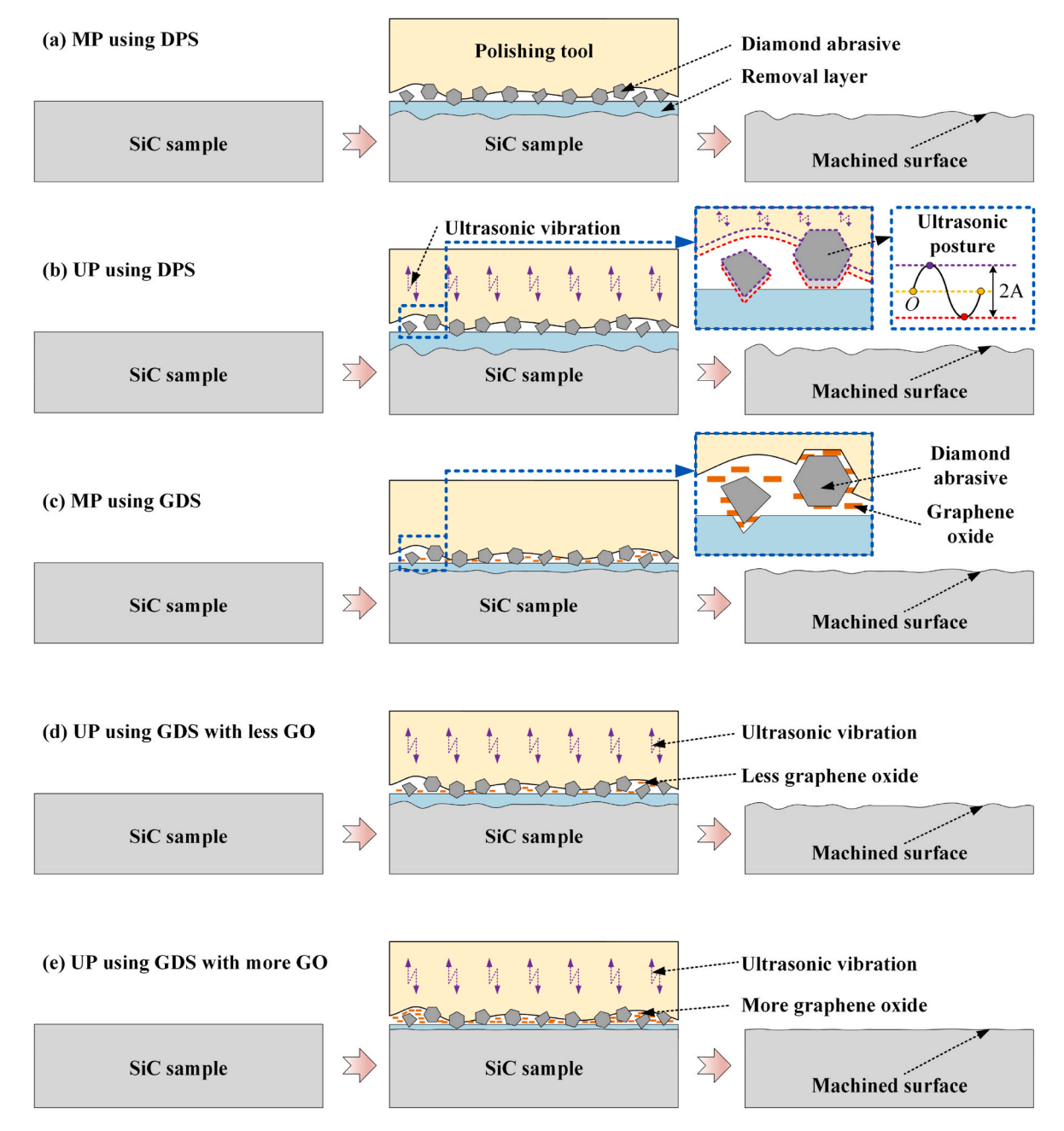


Fig. 10. Material removal mechanisms for (a) MP using DPS, (b) UP using DPS, (c) MP using GDS, (d) UP using GDS with less GO, and (e) UP using GDS with more GO.

slurries exhibited superior polishing performance on surface quality compared to traditional diamond polishing slurries. A surface roughness improvement of 31.62% was achieved on the surface after ultrasonic polishing using 0.1GDS. As the GO concentration increased, the surface roughness and MRR decreased, with significantly smoother surface and fewer scratches, fluctuations, and pits. This is probably attributed to the fact that more graphene oxide effectively enhances the lubrication characteristics among the polishing tool, diamond abrasives and sample surfaces, which in turn reduces the wear and COF between the abrasives and samples. In addition, the high frequency of ultrasonic vibration effectively increased the MRR of SiC polishing by 18.3% compared to MP, mainly due to the higher impact kinetic energy and cutting speed of abrasives. Meanwhile, ultrasonic vibration also effectively improved the surface quality polished using the GDS. This is because ultrasonic vibration allows for a better uniform distribution of GO and abrasives to further enhance the lubrication characteristics of GO nanosheets. The synergistic use of hybrid slurries and ultrasonic polishing provides a novel perspective for green, efficient and high-precision polishing of ceramic materials.

# CRediT authorship contribution statement

Xin Chen: Conceptualization, Methodology, Software, Formal analysis, Data curation, Validation, Writing—original draft, Writing—review & editing. Yingdong Liang: Software, Investigation. Zhijie Cui: Methodology, Investigation. Chao Zhang: Resources, Project administration. Zixuan Wang: Investigation, Validation. Tianbiao Yu: Supervision, Funding acquisition, Writing—review & editing. Ji Zhao: Supervision, Funding acquisition, Writing—review & editing.

#### Statement of originality

I write on behalf of myself and all co-authors to confirm that the results reported in the manuscript are original and neither the entire work, nor any of its parts have been previously published. The authors confirm that the article has not been submitted to peer review, nor has been accepted for publishing in another journal. The authors confirm that the research in their work is original, and that all the data given in the article are real and authentic. If necessary, the article can be recalled, and errors corrected.

# Declaration of competing interest

The authors declare that they have no known competing financial interests or personal relationships that could have appeared to influence the work reported in this paper.

# Acknowledgments

This work was supported by the Major State Basic Research Development Program of China [Grant No. 2017YFA0701200] and the Post-doctoral Science Foundation of China [Grant No. 2021M700717] and the Fundamental Research Funds for the Central Universities [Grant No. N2103001, No. N2203016]. Besides, Xin Chen would like to appreciate the continuous assistance of Di Song from the School of Science and Yu Huang, Guangjian Fang, Pengkai Wang and Jianing Xu from the School of Resources and Civil Engineering.

### Appendix A. Supplementary data

Supplementary data to this article can be found online at https://doi.org/10.1016/j.ceramint.2022.10.172.

#### References

- [1] B.S. Shin, K.S. Park, Y.K. Bahk, S.K. Park, J.H. Lee, J.S. Go, M.C. Kang, C.M. Lee, Rapid manufacturing of SiC molds with micro-sized holes using abrasive water jet, Trans. Nonferrous Met. Soc. China (English Ed. 19 (2009) s178–s182, https://doi. org/10.1016/S1003-6326(10)60267-1.
- [2] W.L. Zhu, B. Anthony, Investigation of critical material removal transitions in compliant machining of brittle ceramics, Mater. Des. 185 (2020), 108258, https:// doi.org/10.1016/j.matdes.2019.108258.
- [3] S. Hauth, L. Linsen, Cycloids for polishing along double-spiral toolpaths in configuration space, Int. J. Adv. Manuf. Technol. 60 (2012) 343–356, https://doi. org/10.1007/s00170-011-3608-8.
- [4] Q.L. Zhao, Z.Y. Sun, B. Guo, Ultrasonic vibration-assisted polishing of V-groove arrays on hard and brittle materials, Proc. Inst. Mech. Eng. Part B J. Eng. Manuf. 231 (2017) 346–354, https://doi.org/10.1177/0954405415616789.
- [5] V.G. Ralchenko, E.E. Ashkihazi, E.V. Zavedeev, A.A. Khomich, A.P. Bolshakov, S. G. Ryzhkov, D.N. Sovyk, V.A. Shershulin, V.Y. Yurov, V.V. Rudnev, High-rate ultrasonic polishing of polycrystalline diamond films, Diam. Relat. Mater. 66 (2016) 171–176, https://doi.org/10.1016/j.diamond.2016.05.002.
- [6] Z. Xia, F. Fang, E. Ahearne, M. Tao, Advances in polishing of optical freeform surfaces: a review, J. Mater. Process. Technol. 286 (2020), 116828, https://doi. org/10.1016/j.jmatprotec.2020.116828.
- [7] J. Zhao, J. Zhan, R. Jin, M. Tao, Oblique ultrasonic polishing method by robot for free-form surfaces, Int. J. Mach. Tool Manufact. 40 (2000) 795–808, https://doi. org/10.1016/S0890-6955(99)00112-1.
- [8] Q. Zhao, Z. Sun, B. Guo, Material removal mechanism in ultrasonic vibration assisted polishing of micro cylindrical surface on SiC, Int. J. Mach. Tool Manufact. 103 (2016) 28–39, https://doi.org/10.1016/j.ijmachtools.2016.01.003.
- [9] T. Zhang, C. Guan, C. Zhang, W. Xi, T. Yu, J. Zhao, Predictive modeling and experimental study of generated surface-profile for ultrasonic vibration-assisted polishing of optical glass BK7 in straight feeding process, Ceram. Int. 47 (2021) 19809–19823, https://doi.org/10.1016/j.ceramint.2021.03.320.
- [10] Q. Zhai, W. Zhai, B. Gao, Y. Shi, X. Cheng, Synthesis and characterization of nanocomposite Fe3O4/SiO2 core-shell abrasives for high-efficiency ultrasoundassisted magneto-rheological polishing of sapphire, Ceram. Int. 47 (2021) 31681–31690, https://doi.org/10.1016/j.ceramint.2021.08.047.
- [11] J.Q. Ge, Y.L. Ren, X.S. Xu, C. Li, Z.A. Li, W.F. Xiang, Numerical and experimental study on the ultrasonic-assisted soft abrasive flow polishing characteristics, Int. J. Adv. Manuf. Technol. 112 (2021) 3215–3233, https://doi.org/10.1007/s00170-021-06598-2.

- [12] X. Yang, X. Yang, K. Kawai, K. Arima, K. Yamamura, Ultrasonic-assisted anodic oxidation of 4H-SiC (0001) surface, Electrochem. Commun. 100 (2019) 1–5, https://doi.org/10.1016/j.elecom.2019.01.012.
- [13] X. Yang, X. Yang, H. Gu, K. Kawai, K. Arima, K. Yamamura, Efficient and slurryless ultrasonic vibration assisted electrochemical mechanical polishing for 4H–SiC wafers, Ceram. Int. 48 (2022) 7570–7583, https://doi.org/10.1016/j. ceramint.2021.11.301.
- [14] H.Y. Tam, H.B. Cheng, Y.W. Wang, Removal rate and surface roughness in the lapping and polishing of RB-SiC optical components, J. Mater. Process. Technol. 192–193 (2007) 276–280, https://doi.org/10.1016/j.jmatprotec.2007.04.091.
- [15] K. Holmberg, A. Erdemir, Influence of tribology on global energy consumption, costs and emissions, Friction 5 (2017) 263–284, https://doi.org/10.1007/s40544-017-0183-5
- [16] H. Sun, F. Lei, T. Li, H. Han, B. Li, D. Li, D. Sun, Facile fabrication of novel multifunctional lubricant-infused surfaces with exceptional tribological and anticorrosive properties, ACS Appl. Mater. Interfaces 13 (2021) 6678–6687, https://doi.org/10.1021/acsami.0c21667.
- [17] Q. Wei, T. Fu, Q. Yue, H. Liu, S. Ma, M. Cai, F. Zhou, Graphene oxide/brush-like polysaccharide copolymer nanohybrids as eco-friendly additives for water-based lubrication, Tribol. Int. 157 (2021), 106895, https://doi.org/10.1016/j. triboint.2021.106895.
- [18] M. Yang, C. Li, Y. Zhang, D. Jia, R. Li, Y. Hou, H. Cao, J. Wang, Predictive model for minimum chip thickness and size effect in single diamond grain grinding of zirconia ceramics under different lubricating conditions, Ceram. Int. 45 (2019) 14908–14920, https://doi.org/10.1016/j.ceramint.2019.04.226.
- [19] M. Li, T. Yu, L. Yang, H. Li, R. Zhang, W. Wang, Parameter optimization during minimum quantity lubrication milling of TC4 alloy with graphene-dispersed vegetable-oil-based cutting fluid, J. Clean. Prod. 209 (2019) 1508–1522, https:// doi.org/10.1016/j.jclepro.2018.11.147.
- [20] T. Li, H. Sun, D. Wang, J. Huang, D. Li, F. Lei, D. Sun, High-performance chemical mechanical polishing slurry for aluminum alloy using hybrid abrasives of zirconium phosphate and alumina, Appl. Surf. Sci. 537 (2021), 147859, https:// doi.org/10.1016/j.apsusc.2020.147859.
- [21] S. Jana, A. Salehi-Khojin, W.H. Zhong, Enhancement of fluid thermal conductivity by the addition of single and hybrid nano-additives, Thermochim. Acta 462 (2007) 45–55, https://doi.org/10.1016/j.tca.2007.06.009.
- [22] J. Leng, T. Guo, M. Yang, Z. Guo, Z. Fang, Z. Liu, D. Li, D. Sun, Analysis of low-velocity impact resistance of carbon fiber reinforced polymer composites based on the content of incorporated graphite fluoride, Materials 13 (2020), https://doi.org/10.3390/ma13010187.
- [23] T. Gao, C. Li, M. Yang, Y. Zhang, D. Jia, W. Ding, S. Debnath, T. Yu, Z. Said, J. Wang, Mechanics analysis and predictive force models for the single-diamond grain grinding of carbon fiber reinforced polymers using CNT nano-lubricant, J. Mater. Process. Technol. 290 (2021), 116976, https://doi.org/10.1016/j. jmatprotec.2020.116976.
- [24] C. Li, X. Li, S. Huang, L. Li, F. Zhang, Ultra-precision grinding of Gd3Ga5O12 crystals with graphene oxide coolant: material deformation mechanism and performance evaluation, J. Manuf. Process. 61 (2021) 417–427, https://doi.org/10.1016/j.imapro.2020.11.037.
- [25] S. Yi, G. Li, S. Ding, J. Mo, Performance and mechanisms of graphene oxide suspended cutting fluid in the drilling of titanium alloy Ti-6Al-4V, J. Manuf. Process. 29 (2017) 182–193, https://doi.org/10.1016/j.jmapro.2017.07.027.
- [26] G. Li, S. Yi, N. Li, W. Pan, C. Wen, S. Ding, Quantitative analysis of cooling and lubricating effects of graphene oxide nanofluids in machining titanium alloy Ti6Al4V, J. Mater. Process. Technol. 271 (2019) 584–598, https://doi.org/ 10.1016/i.jmatprotec.2019.04.035.
- [27] S. Huang, X. Li, D. Mu, C. Cui, H. Huang, H. Huang, Polishing performance and mechanism of a water-based nanosuspension using diamond particles and GO nanosheets as additives, Tribol. Int. 164 (2021), 107241, https://doi.org/10.1016/ itriboint.2021.107241
- [28] X.B. Hu, Y. Yu, J.E. Zhou, L.X. Song, Effects of process parameters on the particle size distribution of graphene oxide aqueous dispersion, Adv. Mater. Res. 750–752 (2013) 1113–1116. https://doi.org/10.4028/www.scientific.net/AMR.750
- [29] H.K. Liu, C.C.A. Chen, C.J. Chen, Effect of graphene additions on polishing of silicon carbide wafer with functional PU/silica particles in CMP slurry, Funct. Mater. Lett. 12 (2019) 1–5, https://doi.org/10.1142/S1793604719500668.
- [30] P. Wu, X. Chen, C. Zhang, J. Luo, Synergistic tribological behaviors of graphene oxide and nanodiamond as lubricating additives in water, Tribol. Int. 132 (2019) 177–184, https://doi.org/10.1016/j.triboint.2018.12.021.
- [31] J.G. Song, L.M. Zhang, J.G. Li, J.R. Song, Influence of ultrasonic on the dispersibility of ZrB2 particles, Mater. Manuf. Process. 23 (2008) 98–101, https:// doi.org/10.1080/10426910701524683.
- [32] S. Stankovich, R.D. Piner, S.B.T. Nguyen, R.S. Ruoff, Synthesis and exfoliation of isocyanate-treated graphene oxide nanoplatelets, Carbon N. Y. 44 (2006) 3342–3347, https://doi.org/10.1016/j.carbon.2006.06.004.
- [33] J. Stafford, A. Patapas, N. Uzo, O.K. Matar, C. Petit, Towards scale-up of graphene production via nonoxidizing liquid exfoliation methods, AIChE J. 64 (2018) 3246–3276, https://doi.org/10.1002/aic.16174.
- [34] H. Zhang, T. Guan, N. Zhang, F. Fang, Fabrication of permanent self-lubricating 2D material-reinforced nickel mould tools using electroforming, Int. J. Mach. Tool Manufact. 170 (2021), 103802, https://doi.org/10.1016/j.ijmachtools.2021.103802.
- [35] T. Zhang, Y. Zhao, T. Yu, T. Yu, J. Shi, J. Zhao, Study on polishing slurry waste reduction in polishing monocrystalline silicon based on ultrasonic atomization, J. Clean. Prod. 233 (2019) 1–12, https://doi.org/10.1016/j.jclepro.2019.06.067.

- [36] T. Yu, X. Guo, Z. Wang, P. Xu, J. Zhao, Effects of the ultrasonic vibration field on polishing process of nickel-based alloy Inconel718, J. Mater. Process. Technol. 273 (2019), https://doi.org/10.1016/j.jmatprotec.2019.05.009.
- [37] T. Yu, T. Zhang, X. Yu, X. Yang, J. Sun, Study on optimization of ultrasonic-vibration-assisted polishing process parameters, Meas. J. Int. Meas. Confed. 135 (2019) 651–660, https://doi.org/10.1016/j.measurement.2018.12.008.
- [38] Y. Ichida, R. Sato, Y. Morimoto, K. Kobayashi, Material removal mechanisms in non-contact ultrasonic abrasive machining, Wear 258 (2005) 107–114, https://doi. org/10.1016/j.wear.2004.05.016.
- [39] Y. Liang, C. Zhang, X. Chen, T. Zhang, T. Yu, J. Zhao, A. Yu, Modeling and analysis of the material removal rate for ultrasonic vibration-assisted polishing of optical glass BK7, Int. J. Adv. Manuf. Technol. 118 (2022) 627–639, https://doi.org/ 10.1007/s00170-021-07967-7.
- [40] W. Xia, J. Zhao, H. Wu, X. Zhao, X. Zhang, J. Xu, S. Jiao, X. Wang, C. Zhou, Z. Jiang, Effects of oil-in-water based nanolubricant containing TiO2 nanoparticles in hot rolling of 304 stainless steel, J. Mater. Process. Technol. 262 (2018) 149–156, https://doi.org/10.1016/j.jmatprotec.2018.06.020.
- [41] W. Shao, X. Liu, H. Min, G. Dong, Q. Feng, S. Zuo, Preparation, characterization, and antibacterial activity of silver nanoparticle-decorated graphene oxide nanocomposite, ACS Appl. Mater. Interfaces 7 (2015) 6966–6973, https://doi.org/10.1021/acsami.5b00937.
- [42] H. Kinoshita, Y. Nishina, A.A. Alias, M. Fujii, Tribological properties of monolayer graphene oxide sheets as water-based lubricant additives, Carbon N. Y. 66 (2014) 720–723, https://doi.org/10.1016/j.carbon.2013.08.045.